

Analysis and Design of ITER 1 MV Core Snubber

This content has been downloaded from IOPscience. Please scroll down to see the full text.

2012 Plasma Sci. Technol. 14 1017

(<http://iopscience.iop.org/1009-0630/14/11/11>)

View [the table of contents for this issue](#), or go to the [journal homepage](#) for more

Download details:

IP Address: 114.255.122.18

This content was downloaded on 15/03/2014 at 01:45

Please note that [terms and conditions apply](#).

Analysis and Design of ITER 1 MV Core Snubber*

WANG Haitian (王海田)^{1,2}, LI Ge (李格)²

¹China Electric Power Research Institute, Beijing 100192, China

²Institute of Plasma Physics, Chinese Academy of Sciences, Hefei 230031, China

Abstract The core snubber, as a passive protection device, can suppress arc current and absorb stored energy in stray capacitance during the electrical breakdown in accelerating electrodes of ITER NBI. In order to design the core snubber of ITER, the control parameters of the arc peak current have been firstly analyzed by the Fink-Baker-Owren (FBO) method, which are used for designing the DIID 100 kV snubber. The $B-H$ curve can be derived from the measured voltage and current waveforms, and the hysteresis loss of the core snubber can be derived using the revised parallelogram method. The core snubber can be a simplified representation as an equivalent parallel resistance and inductance, which has been neglected by the FBO method. A simulation code including the parallel equivalent resistance and inductance has been set up. The simulation and experiments result in dramatically large arc shorting currents due to the parallel inductance effect. The case shows that the core snubber utilizing the FBO method gives more compact design.

Keywords: international thermonuclear experimental reactor (ITER), neutral beam injector (NBI), $B-H$ curve, core snubber, eddy current, arc current, eddy current loss, hysteresis loss

PACS: 85.70.Ay

DOI: 10.1088/1009-0630/14/11/11

1 Introduction

The neutral beam injector (NBI) system of the International Thermonuclear Experimental Reactor (ITER) includes a high power ion source, a high voltage power supply (HVPS), a neutral beam transmission subsystem, a vacuum subsystem and so on [1~3]. High energy neutral beam injection is a highly efficient technique for plasma heating and current drive in tokamaks. As the accelerator grid operates at a high electric field and works under different conditions, the ion sources in NBI frequently suffer from electrical breakdown, which is defined as short circuit in the field of electrical science. In order to prevent the ion source from malfunctions or permanent damage, the short-circuit current should be less than 3 kA, and the absorbed energy on its ion source electrodes must be less than 10 J [4]. The core snubber as a protection system is usually inserted between the ion source and the acceleration power supply as seen in Fig. 1 [5]. The core snubber is shown in Fig. 2, where i_A is the arc current, r_1 and r_o are the inner radius and outer radius respectively, N_c , N_L , N_T are the number of cores, magnetic tape layers of each core, and conductor turns, and W is the width of each core. The work principle of the snubber is that it can suppress the short-circuit current by its impedance, and can absorb the discharging energy by its equivalent resistor.

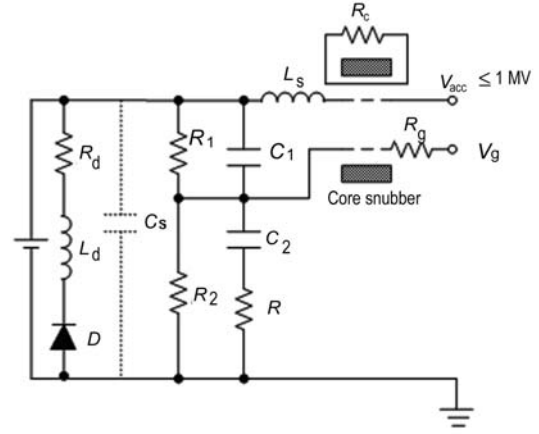


Fig.1 The schematic diagram of EAST NBI power supply system

As in Ref. [6], the simplified equivalent circuit of the core snubber consists of the parallel resistance R and inductance L when neglecting its leakage inductance. It has two key elements which depend on the frequency of the applied source. These parallel components are adopted rather than series components, because the effective shunt resistance varies less than the effective series resistance with high frequency excitation. The core snubber absorbs the capacitive stored energy by iron losses, mainly by eddy current loss [7~9]. Fink-Baker-Owren (FBO) presented the analysis method for

*supported by National Program on Key Basic Research Project of ITER Core Snubber in China (973 Program) (No. 2010GB108003)

the core snubber on the assumption that the core snubber never saturates and the magnetization inductance is an infinitely large quantity [7]. The design of the core snubber for DIIIID 100 kV referred to the FBO method. With the secondary resistor, the capability of the snubber system to absorb energy can be improved [10~12]. In fact, the inductance is in real existence in the equivalent circuit of the core snubber, and the hysteresis loss is also existent. In this paper, we analyze the topological structure of the core snubber first. Secondly, the characteristic parameters of the Fe-based nanocrystalline soft magnetic materials (FINEMET) are obtained, and the hysteresis loss is computed. Then, the simulation model including the parallel inductance is set up. Finally, the scheme of the 400 pF/1 MV core snubber based on the mini core snubber is determined by the simulation model.

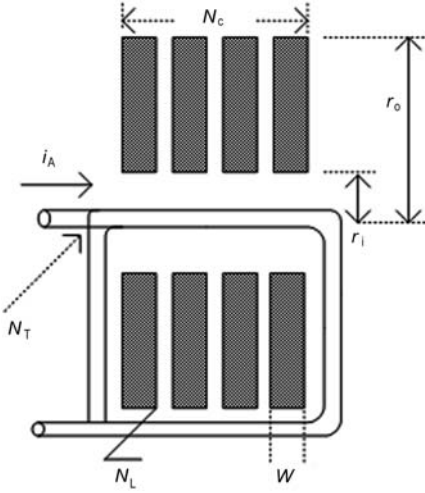


Fig.2 The configuration of core snubber

2 Topological structure of the core snubber

Fig. 3 shows the stray capacitance C_s and the equivalent time-varying resistance R_s of the core snubber [7]. Neglecting its shunt inductance, FBO [7] presented the analytical form of R_s , which is

$$R_s = \frac{5N_c N_L N_T^{3/2} \rho W}{\pi r_1 [1 + (r_o/r_1)^{1/2}] (\rho C V_0)^{1/2}} \coth\left(\frac{t}{2T_0}\right), \quad (1)$$

where ρ is the resistivity of the tape metal, B is the swing of magnetic flux density of the FINEMET core material, which equals the residual density B_r plus saturation flux density B_s . The discharge time constant T_0 is [7,9]

$$T_0 = \frac{5N_c N_L N_T^{3/2} W}{[1 + (r_o/r_1)^{1/2}] (\pi r_1 V_0)} \left(\frac{B\rho C}{\pi r_1 V_0}\right)^{1/2}. \quad (2)$$

The discharged peak current of the arc is [7,9]

$$\hat{i}_A = 0.385 C V_0 / T_0. \quad (3)$$

Due to $N_T=1$ in the ITER NBI system, Eq. (2) can be rewritten as

$$T_0 = \frac{5L(r_o - r_1)S_f}{d[1 + (r_o/r_1)^{1/2}]} \left(\frac{B\rho C}{\pi r_1 V_0}\right)^{1/2}, \quad (4)$$

where d is the thickness of the magnetic tape, S_f is the packing factor of the core snubber, L is the length of the core snubber, which equals $N_c W$.

From Eqs. (1) and (4), we can see that the equivalent time-varying resistance R_s and the time constant T_0 are proportional to the length of the core snubber, and that the peak current of the arc current is inversely proportional to the length of the core snubber. In order to raise the material utilization ratio, we should choose which kind of structure between slender core snubber and stubby core snubber.

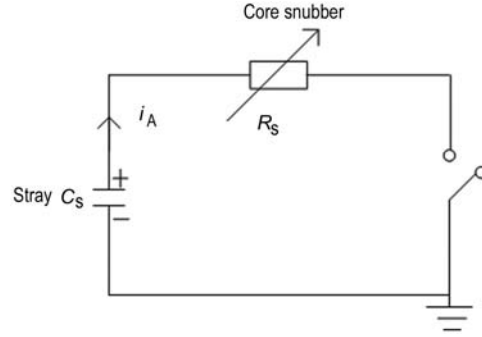


Fig.3 The simplified circuit of core snubber

2.1 Modification of inner and outer radii of core snubber

We assume that d , W , L and r_o/r_1 are constant. If a proportion factor $k > 0$ and $r_1 \rightarrow kr_1$, we have $r_o \rightarrow kr_o$ and $N_L \rightarrow kN_L$. Now the equivalent variable resistance R'_s is

$$R'_s = \frac{5N_c k N_L N_T^2 \rho W}{\pi k r_1 [1 + (r_o/r_1)^{1/2}] (N_T \rho C V_0)^{1/2}} \frac{(\pi B k r_1)^{1/2}}{(\pi k r_1 V_0)^{1/2}} = \sqrt{k} R_s. \quad (5)$$

And the discharge time constant T'_0 is

$$T'_0 = \frac{5Dk(r_o - r_1)S_f}{d[1 + (r_o/r_1)^{1/2}]} \left(\frac{B\rho C}{\pi k r_1 V_0}\right)^{1/2} = \sqrt{k} T_0. \quad (6)$$

From Eqs. (5) and (6), we find that the equivalent variable resistance and discharge time constant are proportional to the square root of the scale factor k . From Eq. (3), we can see that the peak current of the arc is inversely proportional to the square root of the scale factor k . And the consumable core material of the core snubber is of the ratio to square of the scale factor k .

2.2 Modification of length of core snubber

In this case, only the length of the core snubber L is changed to kL , and the other dimensions of the core snubber are still constant. From Eqs. (3), (5) and (6), we can find that the peak current, equivalent variable resistance and discharge time constant are the same as

the corresponding ones in section 2.1. The consumable core material of the core snubber is also the ratio to the scale factor k . Therefore, from the point of view of saving material, we find that the topological structure of the core snubber is better in a slender structure than in a stubby structure.

3 Characteristics of the magnetic cores

The magnetization of the mini core snubber with reversal residual magnetization, N_t turns winding, an effective cross-sectional area A_c , and an average magnetic path length l_e can be described by relating the electrical quantities of the winding and the field quantities of the mini core snubber,

$$B_t = \frac{1}{N_t A_c} \int v(t) dt - B_r, \quad (7)$$

$$H = \frac{N_t}{l_e} i, \quad (8)$$

where v is the voltage across the winding, i is the current through the winding, B_t is the magnetic induction, H is the magnetic field strength, l_e equals multiplying π by the sum of r_1 and r_0 .

3.1 Confirmation of residual density

The residual density B_r can be obtained by two methods. One is obtained from the manufacturer of the FINEMET core material, and the other is obtained by an experimental method. Here, the experimental method is introduced. A simplified schematic of the experimental circuit is shown in Fig. 4. It consists of three switches (K_1 , K_2 , K_3), a core snubber, a capacitance, an adjustable voltage source, an adjustable current source, a current transformer, a divider voltage probe and an oscilloscope. The capacitance can be charged by the adjustable voltage source. I_{bias} can be adjusted by the current source. The oscillograph can record the voltage waveform and current waveform of the discharge pulse. Based on this experimental circuit, the residual magnetic flux density B_r can be obtained by referring to the procedure as follows:

a. I_{bias0} is determined. In order to keep the core snubber in reverse residual magnetization, the minimum reverse magnetizing current I_{bias0} should be determined first. B_r and the magnetic intensity H_0 should satisfy

$$B_r = \mu H = \mu_{r0} \mu_0 H, \quad (9)$$

where μ is the total permeability of the FINEMET that defines the slope of the $B-H$ curve, μ_{r0} is the relative permeability of the FINEMET and μ_0 is the permeability of air $\mu_0 = 4\pi \times 10^{-7} \text{ T} \cdot \text{m/A}$. According to Eqs. (8) and (9), I_{bias0} should satisfy

$$I_{bias0} \geq \frac{B_r l_e}{\mu_{r0} \mu_0 N_t}. \quad (10)$$

b. A half part of the $B-H$ curve should be plotted. For the record-data of the voltage waveform and current waveform, we use Eqs. (8) and (7) taking no account of B_r , and plot a half part of the $B-H$ curve as shown in Fig. 5(a). Point a is determined by the first pair sample data of the voltage waveform and current waveform. Point b corresponding to the same pair sample data is on the upward side of point a. In order to determine point b, this $B-H$ curve may be plotted repeatedly.

c. B_r can be obtained. According to the characteristics of the $B-H$ curve, the length of line \overline{ab} quantitatively equals $2B_r$. Consequently, point a and point b can be expressed as $(0, -B_r)$ and $(0, +B_r)$ respectively. And the $B-H$ curve derived is shown in Fig. 5(b).

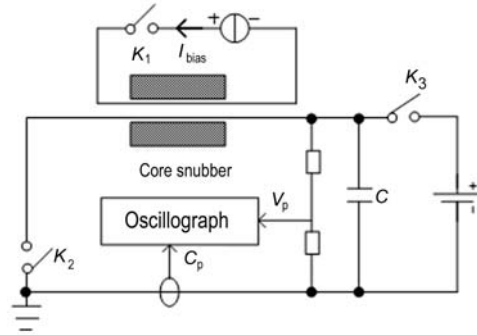
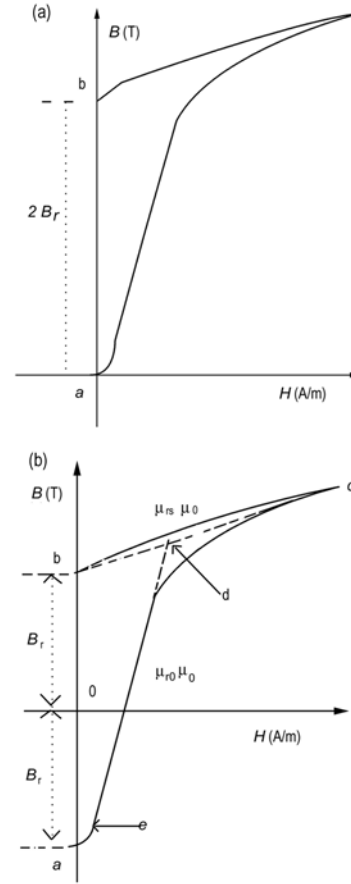


Fig.4 Simplified schematic of experimental circuit



(a) Without regard to B_r , (b) With regard to B_r

Fig.5 Sketch map of a half part of $B-H$ curve (color on-line)

3.2 B - H curve and characteristics of the magnetic cores

The test mini core snubber consists of 3 cores. The dimensions of each core are 170 mm in inner diameter, 240 mm in outer diameter, 30 μm in tape thickness and 50 mm in tape width. The material is the FINEMET. The capacitance C_s is 76 nF. The current i is measured with a current transformer. The voltage v across a 4-turn winding is measured with a high-voltage probe. The data are collected at the highest rate of a 2 GS/s digital oscilloscope. According to the dimensions of the core snubber and B_r provided by the manufacturer, the bias current $I_{\text{bias}0}$ is about 25 A. Considering the possible error, we choose $I_{\text{bias}0}$ for about 50 A. It should be noted that, before turning on K_2 , K_1 should be switched off. The measured voltage and current pulses on the test stand are shown in Fig. 6. The B - H curve can be obtained using Eqs. (7) and (8), and the typical curve is shown in Fig. 7.

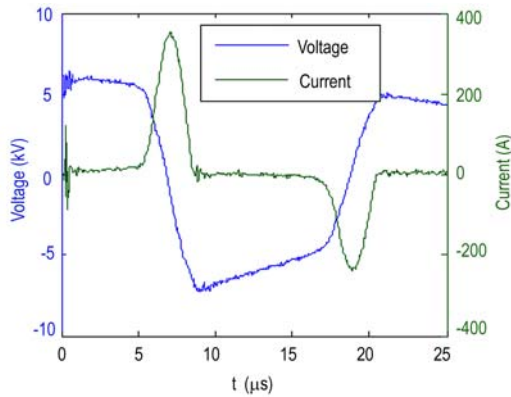


Fig.6 Voltage and current waveform recorded by oscilloscope (color online)

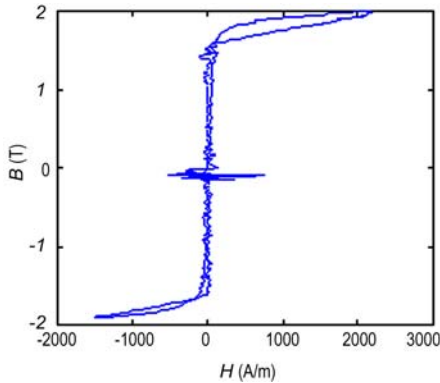


Fig.7 Typical B - H curve (color online)

The non-saturation inductance of the mini core snubber is

$$L = \frac{N_t^2 A_c}{l_e} \frac{dB_t}{dH}, \quad (11)$$

where dB_t/dH , correspondence non-saturation inductance, equals the slope of line \overline{ed} as shown in Fig. 5(b).

The unsaturated inductance of the mini core snubber with 4-turn winding is about 1 mH when it is magnetically unsaturated. According to Fig. 7 and Eq. (11),

the key parameters of the mini core snubber can be obtained as listed in Table 1. As in Ref. [13], Cao L and Li G found that the major loop area of the parallelogram equals that of the B - H rectangular loop, and presented a method for the hysteresis loss $Loss_h$ calculation, which equals the product of the area of the hysteresis loop and the volume of the hysteresis ring,

$$Loss_h = \frac{4\mu_{r0}}{\mu_{r0} - \mu_{rs}} B_r H_c A_c l_e, \quad (12)$$

where μ_{rs} and μ_{r0} are the magnetic saturated and unsaturated relative permeability respectively, and their corresponding quantities equal the slope of line \overline{dc} and \overline{ed} as seen in Fig. 5(b) divided by μ_0 .

Table 1. Key parameters of the core snubber

Core material	Value
Saturation flux density B_s (T)	1.25
Residual density B_r (T)	0.3
Coercive force H_c (A/m)	20
Magnetic unsaturation relative permeability μ_{r0}	8500 (200 kHz)
Magnetic saturation relative permeability μ_{rs}	160

According to the dimensions of the test mini core snubber and parameters listed in Table 1, the hysteresis loss is about 0.1 J, and it is nearly 7% of the stored energy in the charging capacitor (76 nF/6 kV). This result shows that the eddy current loss is the main part of the total iron loss.

4 Test and simulation of mini core snubber

In the experiment, the core snubber is the same as the one in section 3, where $N_t=1$, $C_s=26.5$ nF, initial voltage $V_0=2.2$ kV. The waveforms of the voltage and discharge current of C_s are shown in Fig. 8, and the discharge current referring to the FBO method is shown in Fig. 8 also. If the first turn of the tape is not fully saturated, the tape thickness should meet [7]

$$d_0 \geq \left(\frac{10N_t \rho C_s V_0}{\pi B r_1} \right)^{1/2}. \quad (13)$$

According to Eq. (13) and experimental conditions, we have $d_0=30.4$ μm . This means that the first turn of the tape is nearly fully saturated. For the comparison between the measured current and the calculated current referring to the FBO method, we found that the two peak values of the current are nearly equal. This means that two curves agree well.

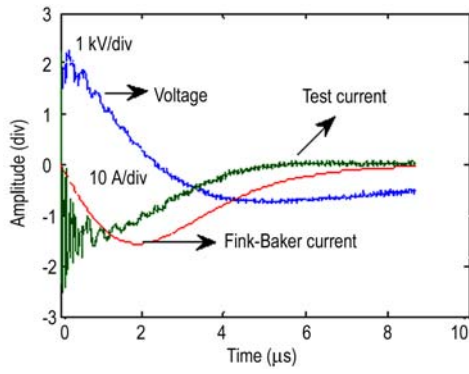


Fig.8 The discharge voltage and current waveform of core snubber (color online)

Fig. 9 shows the discharged current and voltage pulses for the increased 4.4 kV charging voltage, and LC oscillation mode occurs in this condition which increases the peak current significantly. The test peak current is about 90 A, and the calculated peak current is about 44 A, which is about one-half of the test value. Accordingly to Eq. (13), we have $d_0=43.4 \mu\text{m}$. This means that the first turn of the tape is already fully saturated. The effective layer of the core snubber is decreased, and so is the parallel inductance L , and the effect of the inductance neglected by FBO is more obvious.

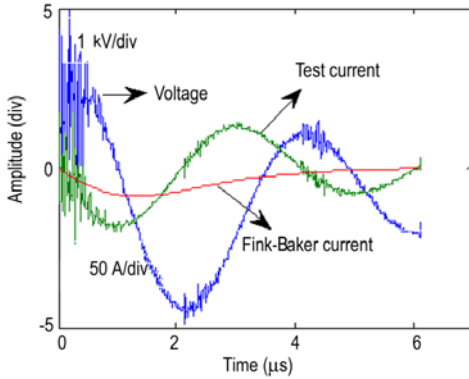
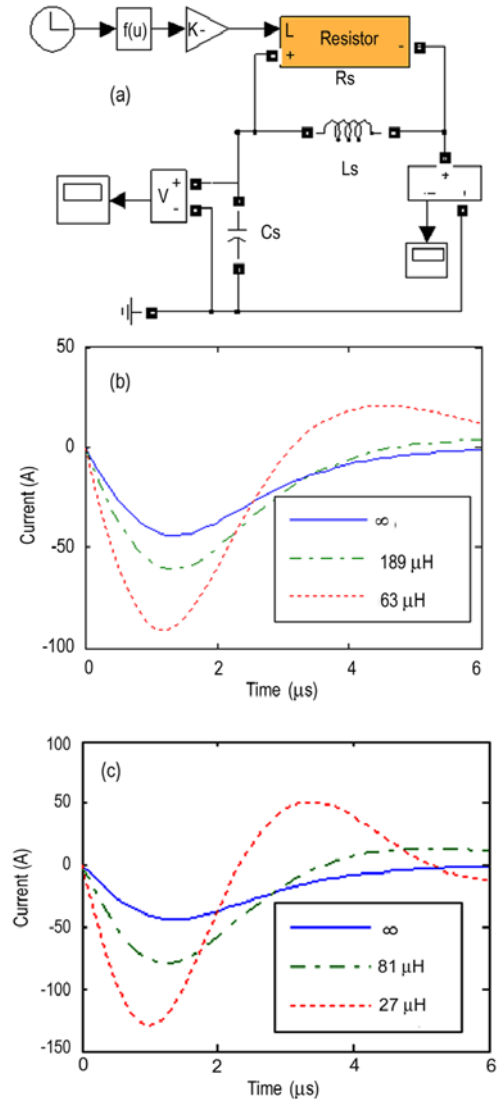


Fig.9 The discharge voltage and current waveforms of core snubber (color online)

In this study, our simulation model consists of the parallel resistance and inductance as seen in Fig. 10(a). The resistance is a variable resistance indicated by the FBO method. The parallel inductance of the core snubber with the FINEMET material is measured by Accuracy Inductance Bridge. The measured inductance is $189 \mu\text{H}$ with a 100 kHz actuating signal, which is fully unsaturated inductance. Another measured inductance is about $63 \mu\text{H}$ ($1 \text{ mH}/16$), which is magnetization inductance by a high magnetizing current, and it is proportional to the relative permeability. The FINEMET magnetic material with the higher inductance and higher saturation magnetic flux density was confirmed to be the most favorable core material for the compact core snubber in the NBI power supply systems [12]. Therefore, the upper limit and lower limit of the parallel inductance with 200 kHz pulse excitation

are $189 \mu\text{H}$ and $63 \mu\text{H}$, respectively. However, the magnetic non-saturation relative permeability μ_{r0} of the FINEMET with 1 MHz pulse excitation is 3500 [12], and the upper limit and lower limit of the parallel inductance are $81 \mu\text{H}$ and $27 \mu\text{H}$ respectively. The simulation waveforms of the arc current corresponding to Fig. 9, considering three cases of parallel inductance of 200 kHz and 1 MHz pulse excitation, are respectively shown in Fig. 10(b) and (c).

From Fig. 9 and Fig. 10(b), considering $63 \mu\text{H}$ parallel inductance, we find that the peak of the measured arc current in Fig. 9 nearly equals the peak of the simulated one in Fig. 10(b). Because the equivalent resistance of the Fink-Baker method is greater than that of considering fully saturated inner layer tapes, the simulated arc current can attenuate faster than the test one. Fig. 9 and Fig. 10(b) also validate that the simulated arc current attenuates faster than the test one.



(a) Simulation model, (b) Simulation arc current with relative permeability $\mu_{r0} = 8500$, (c) Simulation arc current with relative permeability $\mu_{r0} = 3500$

Fig.10 Simulation model and simulation arc current (color online)

5 Comparison of the designed scheme with reference design for ITER

The stray capacitance of the ITER NBI system is about 400 pF, and the operating voltage is 1 MV [12]. The absorbed energy on the ITER ion source electrodes must be less than 10 J. WATANABE et al. presented a design base for the core snubber in the ITER NBI system [12]. At present, this design base as the reference design has been determined by ITER officials for the core snubber of ITER NBI. And the design of the core snubber in the DIID NBI system is based upon the FBO method. The reference design and FBO method are different mechanics. The former is based on the parallel inductance whereas the latter is based on the equivalent time-varying resistance neglecting the parallel inductance. Therefore, it is very difficult to make a logical comparison for the two typical methods. In this paper, we assume that the core is of the same dimensions as one in Ref. [12], except that the tape thickness d is 30 μm . Its dimensions and characteristic parameters of the core material are listed in Table 2. We decrease N_c from 13 to 11. And the result means that the size of the core snubber as by the FBO method is less than the size of one as by the WATANABE method.

Table 2. Parameters of ITER NBI

Item	Value
Inner radius r_1 (mm)	200
Outer radius r_0 (mm)	450
Core width W (mm)	25.4
Tape thickness d (μm)	30/20
Number of laminations N_L	5833
Packing factor S_f	0.7
Conductor turns N_T	1
Number of core N_c	11/13
Saturation flux density B_s (T)	1.35
Residual flux density B_r (T)	1.23
Magnetic unsaturation relative	3500 (1 MHz)
Permeability μ_{r0}	
Operating voltage V_0 (MV)	1
Stray capacitance C_s (pF)	400

The inductance is calculated to be 9.7 μH for one core [12]. Therefore, the total inductance of the core snubber is calculated to be 107 μH . The measured unsaturated inductance is about 320 μH , which is about three times as much as the calculated values. The performance of the core snubber can be improved with secondary resistor R_L [10~12]. With low-inductive resistor $R_L=500 \Omega$ and different parallel core snubber inductances, the discharge current pulses of the 400 pF capacitor discharged at 1 MV are shown in Fig. 11.

Fig. 11 shows that the arc current peak referring to the FBO method is almost the same as one by WATANABE (1 MV/500 $\Omega=2000$ A). This shows that the size of the core snubber can be reduced by 2/13 using the Fink-Baker core snubber compared with the WATANABE core snubber. If the ratio of r_0/r_1 is less, the advantage of the FBO method is more obvious.

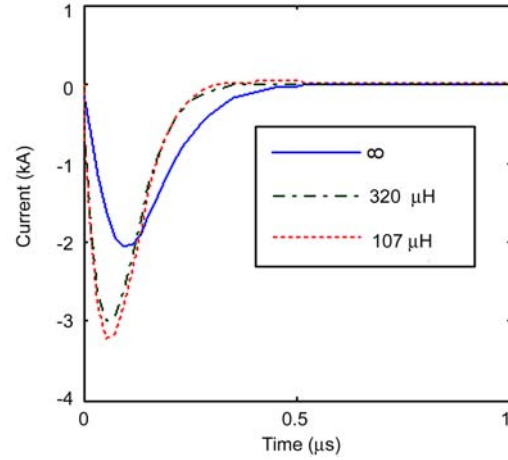


Fig.11 Simulated arc current with different parallel inductances for ITER core snubber (color online)

6 Conclusion

Based on the controlling parameter T_0 of the FBO method for the arc current peak, the relation between the controlling parameter and the topological structure of the core snubber can be derived, and the slender structure for the core snubber has been confirmed. Accordingly to the $B-H$ curve of the mini core snubber, the five key parameters listed in Table 1 can be obtained, and the hysteresis loss can be derived. In this investigation, we have analyzed the effect of the parallel inductance, which is neglected by FBO, and we have set up a simulation model including the parallel equivalent resistance and inductance. Our simulation and experimental results show that the effect of the parallel inductance can increase the arc current obviously. This investigation has improved the FBO method. The core snubber referring to the FBO method is more compact than one referring to the WATANABE method.

References

- 1 Li W. 2009, Research and design of the transmission line and snubber for EAST-NBI high-voltage power supply [Ph.D]. Institute of Plasma physics, Chinese Academy of Sciences, Hefei, China (in Chinese)
- 2 Baruah U K, Patel P J, Bandyopadhyay M, et al. 1997, Power supply system for 1000 s neutral beam injector. Proc. of 17th Symposium on Fusion Engineering, San Diego, California, USA. 2: 1133, IEEE/NPSS
- 3 Alex J, Schminke W. 1997, A high voltage power supply for negative ion NBI based on PSM technology. Proc. of 17th Symposium on Fusion Engineering. San Diego, California, USA. 2: 1063, IEEE/ NPSS

- 4 Watanabe K, Higa O, Kawashima S, et al. 1997, Design of ITER NBI power supply system. Tokai-mura: Japan Atomic Energy Research Institute, JAERI-Tech 97-034
- 5 Matsuoka M, Matsuda S, Nagamura H, et al. 1984, IEEE Trans. Plasma Science, 12: 231
- 6 Wheeler H A. 1942, Proceedings of the Institute of the Radio Eng., 30: 412
- 7 Fink J H, Baker W R, Owren H M. 1980, IEEE Trans. Plasma Science, 8: 33
- 8 Choi J, Namihira T, Sakugawa T, et al. 2007, IEEE Trans. Plasma Science, 35: 1791
- 9 Wang H, Li G, Cao L, et al. 2010, Plasma Science and Technology, 12: 499
- 10 Cao L, Li G, Wang H. 2011, Plasma Science and Technology, 13: 115
- 11 Bigi M, De Lorenzi A, Grandi L. 2009, Fusion Eng. Des., 84: 446
- 12 Watanabe K, Mizuno M, Nakajima S, et al. 1998, Review of Scientific Instruments, 69: 4136
- 13 Cao L and Li G. 2010, IEEE Trans. Energy Conversion, 25: 626

(Manuscript received 19 July 2011)

(Manuscript accepted 24 November 2011)

E-mail address of corresponding author LI Ge:
lige@ipp.ac.cn